PCCP

View Online
Dynamic Article Links

Cite this: *Phys. Chem. Chem. Phys.*, 2011, **13**, 8783–8794

www.rsc.org/pccp

**PERSPECTIVE**

# How many amorphous ices are there?

**Thomas Loerting,*[a] Katrin Winkel,[ab] Markus Seidl,[a] Marion Bauer,[b] Christian Mitterdorfer,[a] Philip H. Handle,[a] Christoph G. Salzmann,[c] Erwin Mayer,[b] John L. Finney[d] and Daniel T. Bowron[de]**

***Received 19th November 2010, Accepted 14th January 2011***
**DOI: 10.1039/c0cp02600j**



Many acronyms are used in the literature for describing different kinds of amorphous ice, mainly because many different preparation routes and many different sample histories need to be distinguished. We here introduce these amorphous ices and discuss the question of how many of these forms are of relevance in the context of polyamorphism. We employ the criterion of reversible transitions between amorphous "states" in finite intervals of pressure and temperature to discriminate between independent metastable amorphous "states" and between "substates" of the same amorphous "state". We argue that the experimental evidence suggests we should consider there to be three polyamorphic "states" of ice, namely low-(LDA), high-(HDA) and very high-density amorphous ice (VHDA). In addition to the realization of reversible transitions between them, they differ in terms of their properties, *e.g.*, compressibility, or number of "interstitial" water molecules. Thus they cannot be regarded as structurally relaxed variants of each other and so we suggest considering them as three distinct megabasins in an energy landscape visualization.

[a] *Institute of Physical Chemistry University of Innsbruck, Innrain 52a, A-6020 Innsbruck, Austria. E-mail: thomas.loerting@uibk.ac.at*
[b] *Institute of General, Inorganic and Theoretical Chemistry, University of Innsbruck, Innrain 52a, A-6020 Innsbruck, Austria*
[c] *Department of Chemistry, Durham University, South Road, Durham DH1 3LE, UK*
[d] *Department of Physics and Astronomy and London Centre for Nanotechnology, University College London, Gower Street, London WC1E 6BT, UK*
[e] *ISIS Facility, Rutherford Appleton Laboratory, Chilton, Didcot, Oxon, OX11 0QX, UK*

## Introduction

Water is ubiquitous and—compared to most other liquids—anomalous. Our planet is called the "blue planet" because water covers about 70% of its surface, and water is regarded as the "molecule of life" because it is vital to all known forms of life. Despite this key role, an understanding of many of its properties has remained elusive. In the solid state the concepts of polymorphism and polyamorphism (amorphous polymorphism) have been established[1] and that water exhibits both phenomena

**Thomas Loerting**

*Thomas Loerting is Associate Professor of Physical Chemistry at the University of Innsbruck (2008–now), where he obtained his PhD degree in Theoretical Chemistry (2000 with K. R. Liedl), and elected member of the Austrian Academy of Sciences ÖAW ("Junge Kurie"). He held a postdoctoral position at the Massachusetts Institute of Technology (2001–2003 with Nobel laureate M. J. Molina). He is directing a research group interested in water and aqueous solutions, with particular emphasis on supercooled water/amorphous ices, ice clouds in the atmosphere and ices in space. He was presented with several awards such as the Nernst–Haber–Bodenstein award by the German Bunsen society and currently holds a Starting Grant by the European Research Council.*

**Katrin Winkel**

*Katrin Winkel studied Physics at the TU Darmstadt, where she worked in the group of Franz Fujara. Since that time her research interest on water, amorphous ice and their relation to ultraviscous liquids arose. In 2005 she moved to the University of Innsbruck and completed her PhD under supervision of Erwin Mayer and Thomas Loerting. Her PhD work about amorphous ice was awarded with the "Karlheinz Seeger Preis 2009" (ÖPG) and the "Georg und Christine Sosnovsky Preis 2010" (Uni Innsbruck). She is currently working at the Institute of Physical Chemistry in Innsbruck as a Hertha Firnberg fellow, funded by the Austrian Science Fund FWF.*

extensively is regarded as one of water's anomalies. The former is an important concept in one-component systems, recognized about 200 years ago from the examples of carbonate, phosphate and arsenate salts.[2,3] The latter is a comparatively novel concept, recognized about 25 years ago with the example of water.[4] It is often related to the hypothesis of the possible existence of more than one liquid phase of composition $H_2O$, possible liquid–liquid immiscibility,[5–7] and the possibility of a (second) liquid–liquid critical point.[8–11] In the case of water an anomalously wide variety of crystalline phases and different amorphous "states"† has been recognized. Some comprehensive reviews have been published in the last decade on these topics.[12–19] However, in the literature there are conflicting views especially on the question how many amorphous states there are. It is the focus of this perspective article to address the key open questions related to distinguishing, defining and identifying amorphous ice states as the basis for counting them.

† There is some difficulty in using the terms "state" and "phase" in the context of the non-crystalline forms of ice as both these terms often carry strong thermodynamic implications of thermodynamic stability. Amorphous ices are clearly metastable structures, so it is advisable to use such terms with caution—hence the use in the early part of this article of quotes where the term "state" is used. From here on, we revert to the use of "state" without quotes, but the reader should note that by using this term we are not implying the forms are thermodynamically stable states.

## The "phase diagram" of non-crystalline water

Depending on the temperature and pressure non-crystalline water may appear as gas, stable liquid, supercooled liquid or as amorphous ice. Fig. 1, derived from a classic figure produced by Mishima,[20] summarizes the approximate $(p,T)$ ranges in which the most stable non-crystalline phases are found at $p < 0.35$ GPa. Liquid water is the stable phase above the melting temperature $T_M$. If care is taken to avoid heterogeneous nucleation (*e.g.*, ice formation at the container surface

**Christoph G. Salzmann**

*Christoph G. Salzmann is a University Lecturer at the Department of Chemistry at Durham University, United Kingdom. He received his PhD in 2004 from the University of Innsbruck (supervisor A. Hallbrucker), Austria. After this, he worked as an Erwin Schrödinger and APART research fellow at the University of Oxford, UK. His research activities focus on structural and materials chemistry. Recent work includes the discovery of ices XIII, XIV and XV, the preparation of a new graphene nanomaterial and the development of a new kind of dispersing agent for carbon nanotubes in water.*

**Erwin Mayer**

*Erwin Mayer retired as Professor of Inorganic Chemistry at the University of Innsbruck (1975–2002), where he obtained his PhD in chemistry in 1963 under supervision of A. Engelbrecht. He held postdoctoral positions at Cornell University (1964–66 with A. W. Laubengayer) and at University of York (1972–73 with R. E. Hester). His major research interests initially were on synthesis and IR/Raman spectroscopic characterization of novel inorganic compounds. Since 1980 he has focussed on calorimetric, structural and spectroscopic studies of water and aqueous solutions. In particular, he developed the hyperquenching technique for vitrification of bulk water and the cryotechnique to isolate crystalline carbonic acid ($H_2CO_3$).*

**John L. Finney**

*John Finney, FRSC, FInstP, is Emeritus Professor of Physics at University College London. His major research interests are in liquids and glasses, with particular reference to water and aqueous solutions, the role of water in biological processes, and the structures of crystalline and amorphous ices. His PhD work on simple liquids was with J. D. Bernal at Birkbeck College London, where he was awarded a personal chair in 1986. He was Head of Neutron Science (1988–93) and Chief Scientist (from 1990) at the ISIS neutron source, and Science Coordinator of the European Spallation Source Project (1993–96).*

**Daniel T. Bowron**

*Daniel Bowron graduated in Physics from the University of Kent at Canterbury in 1991 and remained for a PhD thesis under Bob Newport. In 1994 he went on to a postdoctoral research fellowship under John Finney at University College London. Between 1998 and 2000 he was a beamline scientist at the European Synchrotron Radiation Facility, before returning to the UK to be an instrument scientist at the ISIS neutron source. In 2009 he was promoted to leadership of the facility's Disordered Materials Group and is also lead scientist for the newly constructed Near and Intermediate Range Order Diffractometer.*

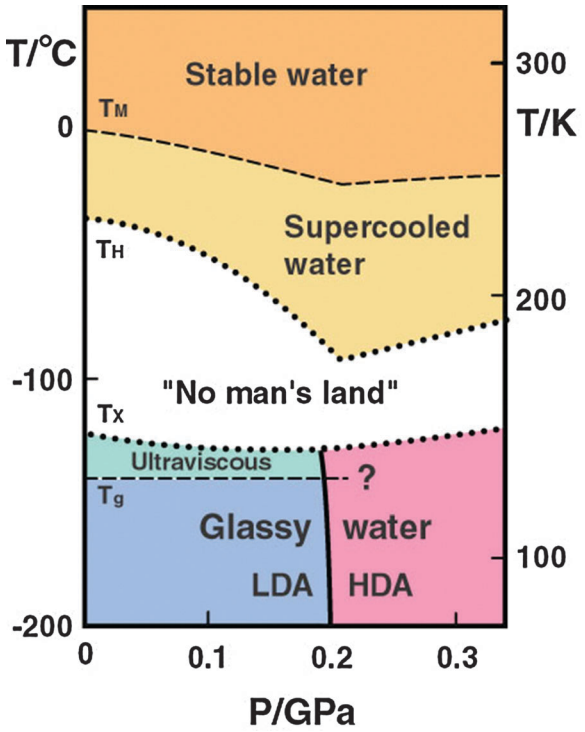


**Fig. 1** Sketch of the "phase diagram" of non-crystalline water. $T_M$: melting temperature, $T_H$: homogeneous nucleation temperature,[23] $T_X$: crystallization temperature,[51] $T_g$: glass-to-liquid transition temperature. $T_g$(1 bar) $\approx$ 136 K;[32,33] it is not clear yet what the value of $T_g$ is at high pressure (horizontal dashed line). Reproduced with modifications from ref. 20.

or induced by the presence of impurities in the sample), liquid water can be obtained below $T_M$. Supercooled water can be formed down to 231 K at ambient pressure[21,22] and down to 181 K at 0.2 GPa.[23] However, even if heterogeneous nucleation is perfectly avoided in experiments, ice forms rapidly below the homogeneous nucleation temperature $T_H$. The "phase diagram" of non-crystalline water would end at $T_H$ were it not for the existence of amorphous ices, the main focus of this article. These amorphous ices can form under suitable conditions below the crystallization line $T_X$. Above $T_X$ amorphous ices crystallize rapidly, and the "phase diagram" of non-crystalline water is blank: the term "No man's land" has therefore been coined for this ($p$,$T$) region. Only crystalline ice can be observed experimentally on the time-scale of milliseconds or longer in the "No man's land". There, metastable (supercooled or glassy) water remains unexplored in experiments of *bulk*, pure water. An experimental characterization would be possible only with ultrafast methods, which are experimentally so demanding that they have so far not successfully been employed for measuring liquid water properties in this temperature range. Instead, computer simulations have been the sole means of investigating through models the possible behaviour of bulk water in "No man's land". It has been proposed that liquid water can be studied experimentally in the "No man's land" in nano-confined environments[24,25] or in the vicinity of interfaces.[26,27] However, we do not consider properties of water deduced from studies in such environments as representative of bulk water properties. Confinement and/or the presence of an interface significantly affect water properties.[28] In particular, phase transitions such as freezing to hexagonal ice may be shifted or suppressed entirely in these environments.[29,30]

It is often suggested that bulk amorphous solids represent low-temperature, kinetically immobilized (vitrified) liquids. This would require amorphous ice to be thermodynamically continuously connected with the supercooled liquid, *i.e.*, that glasses experience a reversible glass-to-liquid transition.[31] A glass-to-liquid transition temperature $T_g \approx 136$ K is determined from calorimetry experiments for (low-density) amorphous ices at 1 bar,[32,33] though this is a matter of lively current controversy. The horizontal $T_g$ line in Fig. 1 is based on the calorimetric $T_g$ at 1 bar. Above this line amorphous ice is regarded as an "ultraviscous liquid" (see Fig. 1). How $T_g$ really depends on pressure is a matter of current research, and so the $T_g$ line ends in a question mark in Fig. 1. Recent volumetric and calorimetric data suggest that low-density amorphous ice (LDA) has a higher $T_g$ than high-density amorphous ice (HDA) and that the $T_g$ of HDA increases with pressure.[34] It is important to distinguish between "true" glasses, and what might be termed "non-glassy amorphous solids". These latter materials may be largely amorphous materials but may contain very small crystallites; or they may even be composed entirely of such micro-crystallites.[35–38] We should note in this context that distinguishing between a "true" glass and a microcrystalline material from X-ray or neutron diffraction patterns is not a trivial exercise. Considering the dynamical behaviour of such systems, while glasses experience a reversible glass-to-liquid transition, "non-glassy amorphous solids" rather re-crystallize and show no glass-to-liquid transition. In the case of water the question of glassy *vs.* non-glassy nature is still debated (see for example chapter 3E in ref. 15), though we note that attempts to interpret high quality neutron diffraction data of several amorphous ices in terms of microcrystalline models were unsuccessful.[39] We emphasize here, however, that there may be glassy amorphous ices and "non-glassy" amorphous ices (as there are in other systems such as silica), depending on the route of their preparation and the thermal history of a particular amorphous ice sample. Unfortunately, this need for a detailed specification of the kind of amorphous ice being considered has resulted in many names and acronyms being used in the literature. In the next section we, therefore, provide an overview about this complex field.

## Acronyms for amorphous ices

The most common acronyms used to describe different variants of amorphous ices are summarized in Table 1. Even though there are also other ways of preparing amorphous ices, we regard amorphous solid water (ASW), hyperquenched glassy water (HGW), low-(LDA), high-(HDA), very high-(VHDA), unannealed high-(uHDA), expanded high-(eHDA) and relaxed high-density amorphous ice (rHDA) as the ones requiring most attention. These acronyms are used in order to indicate how the amorphous ice was made or what its density is and what the sample history was.

The formation of an amorphous solid water was first reported in 1935[40,41] using the route of depositing warm water

**Table 1** Summary of bulk amorphous ice variants encountered in the literature. Amorphous ices produced by the influence of high-energy radiation on crystalline ice (see text) are not listed. Densities quoted are as measured by buoyancy in liquid nitrogen–argon mixtures. Densities obtained using this method are accurate to $\pm 0.01$ g cm$^{-3}$

| | Acronym | Name | Preparation/sample history | Density/g cm$^{-3}$ |
|---|---|---|---|---|
| LDA | ASW | Amorphous solid water | Water vapour deposition[40,41] | 0.94[42] |
| | HGW | Hyperquenched glassy water | Cooling of liquid droplets at $10^7$ K s$^{-1}$ [43] | 0.94[42] |
| | LDA-I | Low-density amorphous ice-I | Heating uHDA at $<0.1$ GPa to 130 K[4,44] | 0.94[42] |
| | LDA-II | Low-density amorphous ice-II | Decompression of VHDA at 140 K to $\leq 0.05$ GPa[44–46] | 0.94[44] |
| HDA | uHDA | Unannealed high-density amorphous ice | Compression of ice Ih at 77 K to $>1.2$ GPa[47] | 1.15[48] |
| | eHDA | Expanded high-density amorphous ice (transforms directly to LDA[49]) | Annealing uHDA at 0.18–0.30 GPa to 130 K[49] | — |
| | | | Decompression of VHDA at 140 K to 0.07 GPa[45,46] | 1.13 |
| | | | Compression of LDA at 130–140 K to $>0.4$ GPa[50] | — |
| | rHDA | Relaxed high-density amorphous ice | Annealing uHDA at 0.3–1.9 GPa[51] | Fig. 5 |
| VHDA | VHDA | Very high-density amorphous ice | Annealing uHDA at $\geq 0.8$ GPa to $>160$ K[48] | 1.26[48] |
| | | | Compression of LDA at $\geq 125$ K to $\geq 1.2$ GPa[52,53] | — |
| | | | Compression of ice Ih at $\geq 130$ K to $\geq 1.2$ GPa[54] | |



vapour on a cold substrate. These deposits are referred to as amorphous solid water (ASW),[55] which is a microporous material highly capable of adsorbing gases.[56–58] In fact, ASW also condenses on interstellar dust particles and is likely the most abundant form of solid water in the universe.[56,59] Therefore, studies on ASW have an astrophysical relevance.[60–64] The number and size of pores depends on the conditions used during preparation, *e.g.*, on the deposition angle or whether or not baffled flow-conditions are employed.[65–69] Annealing the sample to 110 K removes the micropores and produces a reproducible bulk state of amorphous water.[66] It is this annealed form of ASW, which needs to be compared with other amorphous forms of water.[70] In particular, the ambiguities in the literature whether or not ASW experiences a glass-to-liquid transition at 136 K may be explainable by the use of microporous ASW in some studies and annealed ASW in other studies.[71–76]

In addition to starting from water vapour, the liquid can be transformed into an amorphous solid by very rapid cooling. Such rapid quenching is a standard method of glass formation for many substances, both organic and inorganic in nature.[77,78] In fact, it is generally accepted that all liquids can, in principle, be vitrified by cooling. Some liquids can be vitrified quite easily even by slow cooling (“good glass-formers”), whereas others can be vitrified only with difficulties by very rapid cooling (“bad glass-formers”). Water is a particularly bad glass-former and a cooling rate of the order of $10^6$–$10^7$ K s$^{-1}$ is necessary for avoiding crystallization to ice I. Achieving such high cooling rates required the development of new techniques: “hyperquenching” or “splat cooling”. Mayer and Brüggeller were the first to succeed in forming an amorphous ice from the liquid by projecting a thin jet of water into a liquid cryomedium.[79,80] Later, Mayer improved the technique by spraying micrometre-sized droplets onto a solid cryoplate, thus avoiding the use of a cryomedium.[43] The resulting deposit is called hyperquenched glassy water (HGW).

Finally, amorphous solids can also be prepared from the crystalline solid, *i.e.*, ice or from other amorphous solids. When crystalline hexagonal ice (ice Ih) is pressurized melting can occur *e.g.*, at 253 K and 0.2 GPa, since one of water’s anomalies is its negative melting volume, a consequence of which is a negatively sloped melting curve according to the Clausius–Clapeyron equation. If the ice Ih melting curve is extrapolated to lower temperature one would expect melting of ice Ih to occur at pressures exceeding $\sim 1.0$ GPa at 77 K. Indeed, pressure-induced amorphization does take place and high-density amorphous ice (HDA) forms upon compressing hexagonal ice[81] or cubic ice[82] beyond 1.1 GPa. It is debated whether this observation can indeed be interpreted as thermodynamic melting immediately followed by vitrification of the liquid to the HDA glass. Alternatively, it has been suggested that overpressurization of the crystal results in a collapse of its lattice, *i.e.*, mechanical melting producing nanocrystallites.[36] Nowadays, this amorphous solid is called unannealed high-density amorphous ice (uHDA). The density of this amorphous state at 77 K and 1 bar is $1.15 \pm 0.01$ g cm$^{-3}$,[48] while both ASW and HGW show densities of $0.94 \pm 0.01$ g cm$^{-3}$.

By annealing uHDA at 0.1–0.3 GPa another HDA state can be produced, which is called expanded HDA (eHDA).[49] By annealing uHDA to $>160$ K at $\geq 0.8$ GPa a state structurally distinct from HDA can be produced, which is called very high-density amorphous ice (VHDA).[48] The structural change of HDA to an apparently distinct state by pressure annealing was first noticed in 2001.[48] Alternatively, VHDA can be prepared by pressurization of low-density forms of amorphous ice (see below) to $>1.2$ GPa at $\geq 125$ K[52,53] or by pressure-induced amorphization of hexagonal ice at 130 K $< T <$ 150 K.[54] The density of this amorphous state at 77 K and 1 bar is $1.26 \pm 0.01$ g cm$^{-3}$.[48]

Upon heating uHDA to $>115$ K at ambient pressure a further apparently structurally distinct amorphous state is produced. The transition is accompanied by release of heat as indicated from calorimetry experiments[83] and by an expansion of $\sim 25\%$.[4] In Fig. 2 (upper curve) the calorimetry trace obtained from differential scanning calorimetry experiments at a heating rate of 10 K min$^{-1}$ is depicted, which indicates that the transition peaks at 115 K. The resulting state has a density of $0.94 \pm 0.01$ g cm$^{-3}$ and is called low-density amorphous ice (LDA). In a recent neutron diffraction study this sample was named LDA-I,[44] the index “I” being added in order to uniquely define how this particular substate of LDA was prepared. Alternatively, LDA can also be produced by decompressing VHDA in the narrow temperature range of 139–140 K to ambient pressure.[45,46,50] The density of this amorphous state at 77 K and 1 bar is also $0.94 \pm 0.01$ g cm$^{-3}$.[48] The sample recovered after following this route was named LDA-II.[44] Other routes to LDA are possible. In Fig. 2 the calorimetry

 

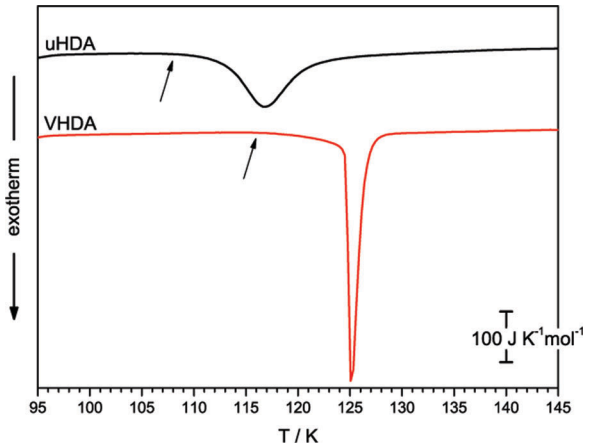


**Fig. 2** Differential scanning calorimetry scans recorded at 10 K $min^{-1}$ for uHDA (top curve) and VHDA (bottom curve). The peak indicates transformation to LDA. Please note that broad enthalpy relaxation precedes the peak. The onset of enthalpy relaxation is indicated by an arrow. The DSC signal is normalized to 1 mol, data are shifted for clarity.

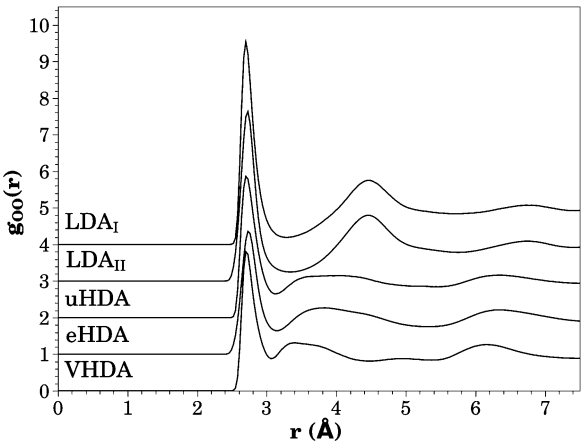


**Fig. 3** Oxygen–oxygen radial distribution functions for five samples of amorphous ice: LDA-I and LDA-II are taken from ref. 44, uHDA and VHDA from ref. 42, eHDA (unpublished data) was prepared by decompressing VHDA to 0.07 GPa[45] Please note the similarity of the LDA-I and LDA-II traces and the similarity of the uHDA and eHDA traces.

trace obtained upon heating a VHDA sample at ambient pressure is shown (lower curve). The exothermic peak indicating transformation of this VHDA sample is shifted by ~10 K (Fig. 2) to higher temperature (compared to the uHDA sample mentioned above). However, again an LDA state results after the transformation. It is unclear presently whether this (third) LDA state is structurally more similar to LDA-I or to LDA-II. As a fourth route heating or decompression of the high-pressure polymorph ice VIII can be employed for producing an LDA sample.[84] A sequential transformation to first HDA and then LDA was observed upon heating ice VIII at 1 bar.[85] Moreover a direct route from ice VIII to LDA has been reported: ice VIII decompressed to 1 bar at 80 K and then heated to 125 K directly transforms to LDA.[86] Furthermore, isothermal pathways by decompression are feasible: by decompressing ice VII or ice VIII at 135 K a transformation directly to LDA is observed using *in situ* Raman spectroscopy in a diamond anvil cell.[87,88] Finally, radiation can be employed to produce LDA. Ice III or ice IX can be amorphized by particle bombardment at electron doses above 2400 electrons $nm^{-2}$,[89] while ice I can be amorphized by keV ion-bombardment at 10–80 K.[90] Similarly, after a dose of a few eV per mole of UV photons, amorphization of ice I can be observed.[91,92]

## Radial distribution functions

A critical and essential difference between amorphous ices and crystalline ices is the absence of long-range periodic order in the former. In fact, and not unexpectedly, the radial distribution function (RDF) of amorphous ices resembles the RDF of liquid water very much more than it resembles the RDF of any of the crystalline polymorphs.[39] One of the main difficulties in counting amorphous ices is their non-equilibrium nature and the slow structural relaxation taking place with time. They are metastable with respect to the thermodynamically stable crystalline polymorph, and their structures cannot be defined using space groups or long-range ordering as a criterion. (Partial) structure factors or (partial) radial distribution functions are employed for analyzing the short- and intermediate-range ordering in these amorphous ices. These can be obtained experimentally using neutron scattering with appropriate isotope substitutions[39,93] combined with empirical potential structure refinement techniques.[94,95] In Fig. 3 a set of five oxygen–oxygen radial distribution functions $g_{OO}(r)$ of differently prepared amorphous ices are depicted. On inspecting the figure one can identify a high similarity between the $g_{OO}(r)$ of LDA-I (prepared by heating a uHDA sample at 1 bar) and LDA-II (prepared by decompressing a VHDA sample to 0.01 GPa at 140 K),[39,44] and also a high similarity between the $g_{OO}(r)$ of uHDA (prepared by pressure-induced amorphization of hexagonal ice at 77 K)[39,42] and eHDA (prepared by decompressing VHDA to 0.07 GPa at 140 K),[45] whereas the $g_{OO}(r)$ of VHDA[42,93] is clearly different from that of any of the other four. Earlier we have shown that the $g_{OO}(r)$ of annealed ASW (prepared by water vapour deposition) and annealed HGW (prepared by hyperquenching of liquid water droplets) are very similar to the $g_{OO}(r)$s of LDA-I and LDA-II.[42] In terms of local coordination the $g_{OO}(r)$ of VHDA implies on average that a water molecule is hydrogen bonded to four approximately tetrahedrally disposed neighbours (a "Walrafen pentamer") with two additional molecules at a similar distance that are *not* directly hydrogen bonded to the central water molecule.[93] These additional molecules have been termed "interstitial" molecules[39] in the sense that they appear to be additional to what one might intuitively expect for the essential underlying random network structure of amorphous ices‡. In contrast, the $g_{OO}(r)$s of the lower density uHDA and eHDA imply an average local coordination of a Walrafen pentamer with only one interstitial water molecule.[39] In Fig. 4a the Walrafen

‡ It is important to note that these "interstitial" molecules are themselves on average similarly 4-fold hydrogen-bond coordinated; *i.e.*, they are themselves fully linked into the essentially tetrahedral random network structure of the system.

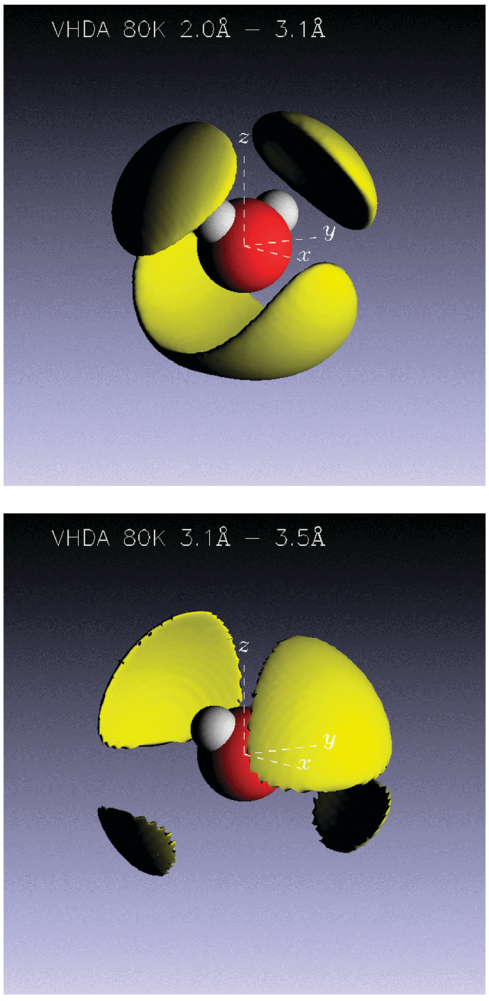


**Fig. 4** (a) First shell of water molecules in the O–O distance range from 2.0 Å to 3.1 Å in the VHDA structure as generated from EPSR refinement of isotope substitution neutron diffraction data. This tetrahedrally arranged shell is accounted for by the first peak in the O–O RDF and corresponds to H-bonded O–O interactions. (b) Location of the interstitial shell of water molecules in the distance range from 3.1 Å to 3.5 Å in the VHDA structure. This is the region of the O–O RDF into which the second neighbour water molecules get pushed as the density of the system increases. The two large lobes in the upper quadrants of the figure show where interstitial water molecules would sit relative to the central molecule, whereas the two smaller lobes in the lower quadrants correspond to where non-bonded water molecules would be if the central molecule is sitting in an "interstitial" site. The plots are generated from the VHDA structural model discussed in ref. 42.

pentamer arrangement is shown using the example of the VHDA structure. For this purpose the density distributions of the water molecules at distances 2.0–3.1 Å from the central water molecule are plotted. At these distances, four water molecules on average surround the central molecule: two above and two below the central water molecule disposed approximately tetrahedrally. However, when plotting water neighbours in the distance range 3.1–3.5 Å (Fig. 4b) the interstitial water molecules become visible while the tetrahedrally hydrogen bonded water molecules of the Walrafen pentamer are not seen: the hydrogen bonded neighbour distances are less than the 3.1 Å cut-off distance used in this plot.

Two water molecules are found in this 3.1–3.5 Å distance range for the VHDA structure. In contrast, the structures of ASW, HGW, LDA-I and LDA-II do not exhibit such interstitial water molecules. However, there are subtle differences in the *intermediate range* order between LDA-I and LDA-II[44] and also between uHDA and eHDA. These differences can be explained in terms of different degrees of relaxation of strain in the structures.[44]

Judging from the RDFs deduced from neutron scattering experiments the amorphous ices mentioned at the outset seem to fall into three structural categories:

- the LDA category (ASW, HGW, LDA-I, LDA-II);
- the HDA category (eHDA, uHDA), and
- the VHDA category (VHDA).

In LDA the first neighbour coordination number (calculated by integrating over the first peak of the $g_{OO}(r)$) is $\sim$4, in HDA it is $\sim$5 and in VHDA it is $\sim$6. Note however that all the RDFs mentioned so far have been obtained from measurements on quench-recovered samples. Klotz *et al*. have deduced the RDFs of pressurized samples using *in situ* measurements, *i.e*., without quenching and without recovering the sample to ambient pressure. These studies suggest that the RDF of VHDA at ambient pressure is highly similar to the RDF of HDA at 100 K and 0.8 GPa, at least up to the second-neighbor shell.[96] These observations are consistent with a strong contraction of the second-neighbor shell being the basis for the transformation from HDA to VHDA and the increase in coordination.

## Structural relaxation

Slow structural relaxation takes place in most amorphous materials, in particular in glasses like window glass. In glasses relaxation is generally observable as an increase in mass density, *i.e*., the glass shrinks as it relaxes. The structural relaxation time depends on temperature. A glass relaxes on the order of minutes or seconds in the vicinity of the glass transition temperature $T_g$, which is $\sim$790 K for Pyrex glass and $\sim$1600 K for $SiO_2$ glass.[97] At a temperature much below $T_g$ relaxation is much slower and may take thousands of years. For a glass that has relaxed well during preparation, its mass density does not change with time. Well relaxed glasses can be prepared by keeping them for hours near the glass transition temperature and may be regarded as "equilibrated" glasses.[98,99] Please note that "equilibrated" here refers to the metastable equilibrium, *i.e*., the crystalline state is still more stable than the (equilibrated) glassy state. Of course, not only the mass density, but also the RDF and other properties change slightly as a glass relaxes. In principle, an endless number of glassy states can be prepared, which differ in terms of the degree of relaxation. However, these differently relaxed glasses are commonly considered to be representatives of the same material. In other words, these differently relaxed glasses are considered to be substates within the same megabasin (which we tentatively here call a "phase") rather than an entirely different "phase" in the energy landscape concept.[100]

## Equilibrating amorphous ices by annealing

In order to judge how many amorphous ices there are, it is necessary to remove the issue of slow relaxation from the

 

discussion. This is not an easy task; perhaps the best way of doing it is by looking at relaxed states of amorphous ices, which are as close as possible to the equilibrated state. Let us first consider the example of high-density amorphous ice (HDA). Mishima *et al*. first observed the formation of HDA by pressure-induced amorphization of hexagonal ice at 77 K and at $p > 1$ GPa.[81] Recently Nelmes *et al*. suggested, with good justification, calling this state unannealed HDA (uHDA).[49] During its preparation the temperature is 77 K at all times. Once hexagonal ice has been amorphized, the relaxation of the strained amorphous solid uHDA is kinetically hindered at 77 K. Handa *et al*. have shown by calorimetry that enthalpy relaxation takes place in uHDA in the range 85–105 K at ambient pressure.[83] This type of relaxation is also observed in the same temperature regime when probing the structure of the sample by diffraction experiments at ambient pressure.[101–103] That is, relaxation takes place even slightly above liquid nitrogen temperature.

Nelmes *et al*. have annealed uHDA at elevated pressure rather than at ambient pressure.[49] Annealing at elevated pressure has the advantage that higher temperature can be reached without major structural transformation of the sample. Nelmes *et al*. have annealed uHDA in the pressure range of 0.1–0.3 GPa up to 130 K and inferred an expansion of the sample as well as a higher thermal stability at ambient pressure.[49] They call this type of material expanded HDA (eHDA), and this material is certainly much better relaxed than uHDA. However, one question remains unanswered: how close to the equilibrated state is eHDA? In order to drive the sample as close as possible to the (metastable) equilibrium, it would be desirable to anneal the sample at higher temperature and/or to allow more time for the sample to relax at higher temperature. Unfortunately this is very difficult in practice and attempts often result in partial or complete crystallization of the sample. Arguably, the amorphous sample is in the most well relaxed state just prior to crystallization. So the best that can be done experimentally to obtain the most relaxed states is to heat the amorphous ices as close as possible to the crystallization temperature. Salzmann *et al*. have developed a technique of determining the mass density of amorphous ices just prior to crystallization.[51] This technique is based on actually crystallizing the sample and subtracting the density jump at crystallization from the well-known density of the crystalline sample. Thus these values represent the densities of experimentally well relaxed samples of amorphous ice. These amorphous samples are called relaxed HDA (rHDA).[51,104] To a large extent, therefore, these data allow the issue of slow relaxation to be eliminated. In Fig. 5 the densities of well relaxed amorphous ices are represented schematically as a function of pressure. In addition to the data provided by Salzmann *et al*.[51] the dependency in the pressure range 0.0–0.2 GPa is shown, estimated from the densities of (low-density) amorphous ice as obtained by compression experiments at 125 K.[52]§ It can be seen that there are three linear regimes of density, which are attributed, respectively, to

§ The density values for HDA and VHDA given in ref. 52 deviate from the densities in Fig. 5 since compression at 125 K results in states far from (metastable) equilibrium.

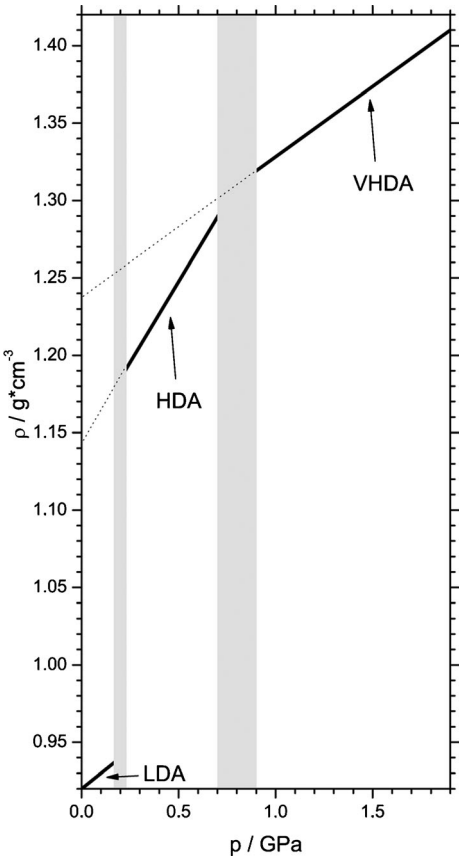


**Fig. 5** Schematic depiction of the densities of well relaxed amorphous ices close to the temperature of their crystallization. The schematic is drawn on the basis of data taken from ref. 51 for rHDA (HDA and VHDA), and estimated from ref. 52 for LDA. The narrow transition region between amorphous "phases" is indicated as a grey shading at ~0.2 GPa for the LDA ↔ HDA transition and at ~0.8 GPa for the HDA ↔ VHDA transition.

low-(LDA),[4] high-(HDA)[81] and very high-density amorphous ice (VHDA).[48] At 0.2 GPa there is an apparent discontinuity in density while at ~0.8 GPa there is a notable change in slope, which is discussed further below.

## Reversible transitions

An apparent discontinuity related to the LDA → HDA transition is also observed when performing quasi-isothermal compression experiments in the temperature range 77–140 K, albeit at higher pressure (> 0.2 GPa) because of the existence of a hysteresis effect.[4,52,53] The transition can even be reversed when performing the decompression at a temperature close to 140 K.[45,50] In decompression experiments the apparent discontinuity is observed at < 0.2 GPa, again with some hysteresis. *In situ* neutron diffraction experiments at 130 K have also been interpreted in favour of a first order-like, discontinuous transition between LDA and HDA.[96] From this point of view it seems beyond doubt that LDA and HDA represent two distinct materials. Nevertheless, the possibility of a very sharp, but still continuous transition cannot be ruled out with certainty from the available experimental findings.[12]

It has also been questioned whether or not HDA and VHDA represent two distinct materials.[12] Annealing of uHDA at >0.8 GPa to $T \approx 160$ K causes further densification and the formation of VHDA.[48] Both uHDA and VHDA transform irreversibly to LDA by heating at ambient pressure, as seen in Fig. 2.[48,81] Several HDA and VHDA substates are experimentally accessible both at high pressure and at ambient pressure. At ambient pressure a broad enthalpy relaxation (exothermic effect) is evident in Fig. 2 for both traces. In the energy landscape concept this can be assigned to the slow relaxation from higher-lying substates to lower-lying substates. On the other hand, the exothermic peak corresponds to the polyamorphic transition from one amorphous "phase" (VHDA or HDA) to another amorphous "phase" (LDA). A polyamorphic transition from VHDA to HDA is not observed in calorimetry experiments at ambient pressure, but rather a broad transition (enthalpy relaxation) from VHDA to HDA-like states.

At high pressure >0.3 GPa Salzmann *et al.* prepared relaxed HDA (rHDA) states by isobaric annealing; these materials have densities higher than that of uHDA (Fig. 2 in ref. 51). The rHDA states obtained on isobaric annealing at $p \geq 0.8$ GPa are called VHDA; this means that there are also VHDA substates.[51] The rHDA states obtained after annealing at 0.1–0.3 GPa are also called eHDA, and the rHDA states obtained after annealing at 0.3–0.7 GPa are called HDA. All rHDA states obtained after annealing at 0.1–0.7 GPa belong to the HDA category. The use of the specific eHDA terminology is justified because eHDA is thought to be the substate directly transforming to LDA.[49] We have argued in a previous publication that it is impossible to tell from the data in Fig. 5 whether there is a discontinuity (involving a density jump close to the experimental uncertainty), a kink or a continuous curve in the vicinity of 0.8 GPa.[105] Here, we want to emphasize that there are two linear regimes, and that the slope in the pressure range 0.2–0.7 GPa differs by approximately 50% from the slope in the pressure range 0.9–1.9 GPa. The slope is closely related to the (quasi-isothermal) compressibility of the material, and apparently the compressibility changes significantly in the vicinity of 0.8 GPa. We, therefore, regard HDA in the pressure range from 0.2–0.7 GPa and VHDA in the pressure range from 0.9–1.9 GPa to be distinct materials of clearly differing compressibility. This assessment is independent of the question whether or not HDA and VHDA are separated by a first order-like transition. In fact, the recent data obtained by Winkel *et al.* on decompressing VHDA at 140 K (close to the crystallization line) clearly shows that there is a finite pressure range (~0.3–0.1 GPa), in which structural states intermediate between HDA and VHDA can be prepared.[45] This is evidence against a first order-like nature of the VHDA → HDA transition and suggestive of a continuous nature of the transition. The key point here is that the continuous transition takes place in a finite and rather narrow pressure range. The material existing above that pressure range is VHDA, and the material below that pressure range is HDA. In the recovered state at 77 K and 1 bar, VHDA is characterized by a density of ~1.26 g cm$^{-3}$, eHDA by a density of ~1.13 g cm$^{-3}$ and LDA by a density of 0.94 g cm$^{-3}$ according to cryo-flotation (buoyancy) measurements.[48] Please note that

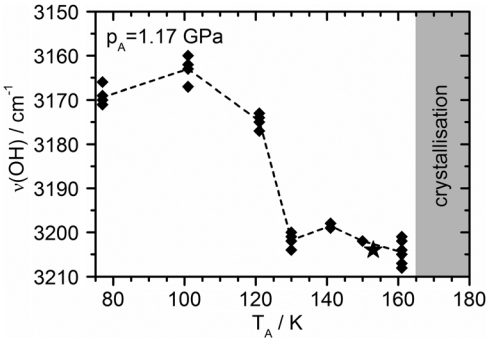


**Fig. 6** Raman observations related to the isobaric HDA → VHDA transition at 1.17 GPa. Raman shift of the coupled OH-stretching vibration in the recovered state at 1 bar indicates a narrow transition in the range 120–130 K. Please note that the frequency shifts by ~35 cm$^{-1}$ in this temperature interval, but no longer shifts above that temperature interval even after keeping the sample for 6 hours at ~153 K and 1.17 GPa (★). Reproduced from ref. 51.

the density of well relaxed eHDA is slightly different from the density of unrelaxed uHDA that is measured to be 1.15 g cm$^{-3}$.[48]

The above-mentioned observation of a narrow range of transformation between HDA and VHDA can also be found when inspecting Raman spectra obtained on isobarically heating uHDA at 1.1 GPa, *i.e.*, when following the originally proposed route for preparation of VHDA.[48] In Fig. 6 the Raman shift of the $\nu$(OH) of samples recovered to 77 K and 1 bar is depicted after they have been brought to different temperatures at 1.17 GPa.[51] The peak position is practically constant at ~3170 ± 10 cm$^{-1}$ in the temperature range from 80–120 K, which corresponds to the peak position in HDA. Also in the temperature range from 130–162 K the peak position is practically constant at ~3205 ± 5 cm$^{-1}$, which corresponds to the peak position in VHDA. In the narrow temperature range 120–130 K the peak position shifts by ~35 cm$^{-1}$, which results from the rather sharp HDA → VHDA transition.

On the other hand no sharp changes are observable at 120–130 K in Fig. 7a (bottom curve) and in Fig. 1B in ref. 48 in a plot of volume change *versus* temperature, when bringing uHDA to 165 K at 1.1 GPa. This apparent discrepancy between Raman data and volumetric data is published in the literature.[48,51] However, an explanation has so far not been given. We, therefore, provide our interpretation here in this perspective article and provide some new data in Fig. 7. We interpret the effect seen in the volume curve as a combined effect. The decrease of sample volume (Fig. 7a, bottom curve) mainly arises from the elimination of (micro)cracks in the sample in the manner discussed by Salzmann *et al.*[51] The decrease of sample volume at 120–130 K expected for the HDA → VHDA transition may be hidden by the densification related to (micro)crack elimination. These (micro)cracks are induced when decompressing ice samples, *e.g.*, uHDA, at 77 K to ambient pressure and remain when recompressing to 1.1 GPa. Samples largely devoid of (micro)cracks, by contrast, show a different compression curve (Fig. 7a, top curve). In this case the absence of (micro)cracks results in an expansion of the sample when heating from 80 K to 130 K at 1.1 GPa.

 

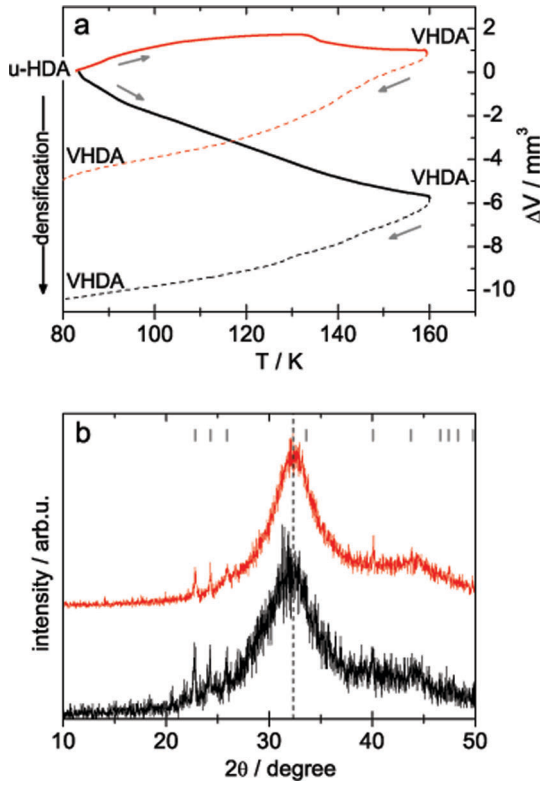


**Fig. 7** (a) Volumetric observations related to the isobaric HDA → VHDA transition at 1.1 GPa. Both curves show volume change *vs.* temperature data upon isobarically heating 300 mg HDA at 1.1 GPa and ~4 K min$^{-1}$. The bottom curve was recorded after decompressing HDA from 1.6 GPa to 1 bar and recompressing to 1.1 GPa at 77 K. The top curve was recorded after decompressing HDA from 1.6 GPa to 1.1 GPa, without bringing the HDA sample in the meantime to ambient pressure. All other experimental parameters are identical for both curves. The difference in the two curves is explained by (micro)cracks, which massively appear upon decompressing to 1 bar, but only to a negligible extent upon decompressing to 1.1 GPa. In the bottom curve the volume effect related to the disappearance of (micro)cracks upon heating obscures a possible volume effect indicating the HDA → VHDA transition. Densification of the sample takes place along the whole heating branch. The bottom curve resembles the curve shown in Fig. 1B in ref. 48. In the top curve the volume effect related to disappearance of (micro)cracks is absent, which results in expansion of the sample at 80–130 K. Densification of the sample sets in above 130 K, which corresponds to the HDA → VHDA transition identified at similar temperature in Fig. 6 by Raman spectroscopy. The samples were quenched to 77 K (dashed lines) and recovered to ambient pressure. (b) Powder X-ray diffractograms of quench-recovered samples recorded at ~80 K using Cu-K$\alpha_1$-rays in $\theta$–$\theta$ arrangement.The calculated peak positions for hexagonal ice are marked by grey ticks, the position of the first halo peak maximum is indicated by a vertical dashed line. The small amount of hexagonal ice arises due to condensation of water vapour during sample handling and transfer.

Above ~130 K densification sets in. When comparing both curves in Fig. 7a one can judge that more than 90% of the densification may be caused by elimination of (micro)cracks, whereas the HDA → VHDA transition merely contributes less than 10%. It is thus essential to study amorphous ice samples free of (micro)cracks in dilatometric studies. Once uHDA data has been prepared by compression of ice I to 1.6 GPa, this can be achieved experimentally by avoiding the depressurization of the samples from 1.6 GPa to ambient pressure followed by recompression to 1.1 GPa. Instead the sample needs to be decompressed from 1.6 GPa directly to 1.1 GPa at a slow rate. In view of the Raman data in Fig. 6, which shows the HDA → VHDA transition at 120–130 K, we interpret this densification observed in Fig. 7a (top curve) above ~130 K as the transition from HDA to VHDA in a narrow temperature range. Indeed, both X-ray diffractograms of the quench-recovered states show the pattern typical of VHDA (Fig. 7b). Thus, we regard the transition between HDA and VHDA as observed by sudden changes in Raman shifts as additional evidence for considering HDA and VHDA as distinct materials. Again, this conclusion would hold even if the transition at 120–130 K was of a sharp, but continuous nature. From the Raman data in Fig. 6 the question of continuity or discontinuity cannot be clarified because no intermediate data points were taken in the interval 120–130 K.

## Two or three amorphous ices?

In Fig. 8 we try to summarize the experimental findings described above and try to construct a simplified potential energy landscape. We focus on three different pressures for which sufficient experimental data are available to aid in the construction of this landscape. The corrugation of the surface indicates that there are a number of substates.

First (left panel of Fig. 8), we consider experiments related to studies of the transformation behaviour of HDA and VHDA by heating them at ambient pressure.[54,83,101–103,106–110] Using this type of approach transient HDA-like states have been observed prior to the sharp transition to LDA. Thermal studies have indicated that there is a sharp, exothermic process related to the HDA → LDA transition,[83] while there is no sharp, exothermic process related to the VHDA → HDA transition. Instead, VHDA continuously transforms to HDA-like states[110,111] and then a sharp transition to LDA is observed (Fig. 2). Thus, at 1 bar VHDA represents a high-lying substate of the HDA megabasin. In the HDA megabasin also uHDA and eHDA can be found. uHDA would occupy substates in the vicinity of the transition state between the LDA and HDA megabasins, and therefore its thermal stability against transformation to LDA is low at 1 bar. An onset temperature of ~108 K can be identified, whereas VHDA shows an onset of ~116 K (arrows in Fig. 2). That is VHDA occupies substates lying lower than the uHDA substates at 1 bar. eHDA represents a well-relaxed state and occupies substates close to the potential energy minimum in the HDA megabasin. Even though its RDF is not much different from the uHDA RDF its thermal stability against transformation to LDA is much higher. Nelmes *et al.* quote an onset transformation temperature of 128 K.[49] Even though there is only one polyamorphic transition at 1 bar, we do not regard this as evidence against the existence of three polyamorphs of ice. As illustrated in Fig. 8 we actually expect the VHDA → HDA transition to be continuous and to resemble a relaxation process at 1 bar because of the unstable nature of VHDA at 1 bar.

Similarly, LDA is unstable at a pressure of, *e.g.*, 1.2 GPa (see the right hand panel of Fig. 8). A hypothetical experiment involving the compression of LDA to 1 GPa at a temperature

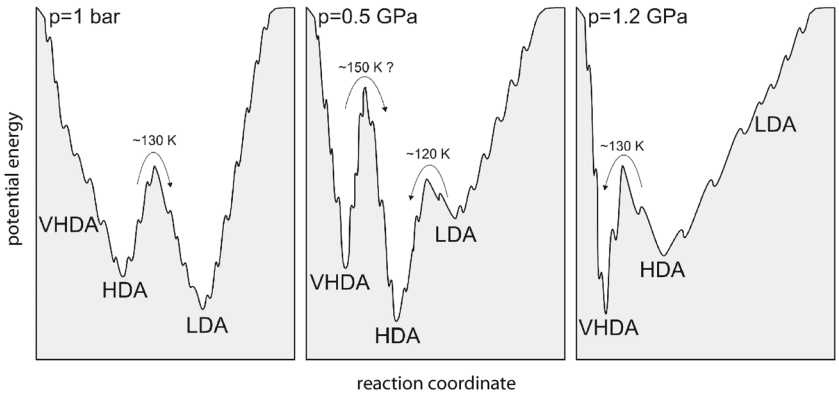


**Fig. 8** Simplified schematic representation of the changes in potential energy surface upon changing pressure. The order of stability of amorphous ices reflects experimental findings. In particular, the HDA → LDA or VHDA → LDA transition at 1 bar takes place at ~130 K in well relaxed HDA or VHDA,[49,54] the upstroke LDA → HDA transition takes place at ~0.5 GPa and ~130 K,[50,52,53] and the HDA → VHDA transition takes place at ~1.2 GPa and ~120 K (see Fig. 6). The reverse transformation VHDA → HDA does not take place at ~0.5 GPa even at 140 K, but below ~0.3 GPa at 140 K.[45,46] The VHDA → HDA transition might take place at ~0.5 GPa and 150 K, and future studies are necessary to clarify this issue. Please note that the energy-landscape seems to comprise only two megabasins at 1 bar (namely LDA and HDA) and 1.2 GPa (namely HDA and VHDA), but three megabasins at 0.5 GPa (LDA, HDA and VHDA). Crystalline polymorphs are omitted for clarity.



close to the absolute zero followed by isobaric heating of LDA at 1 GPa to 160 K might show a slow relaxation from LDA to HDA-like states and subsequently a sharp exothermic event related to the transition HDA → VHDA. It would be desirable to employ *in situ* thermal methods such as differential thermal analysis (DTA) or differential scanning calorimetry (DSC) at ~1.2 GPa. Some of these *in situ* experiments have already been done, namely *in situ* volumetry and Raman spectroscopy on recovered samples after *in situ* annealing at ~1.2 GPa. These experiments (Fig. 5–7) suggest a sharp transformation from HDA to VHDA at ~130 K and ~1.2 GPa. By contrast, LDA is so unstable at 1.2 GPa that it has not been observed in this pressure regime. That is, at 1.2 GPa two amorphous states of ice need to be distinguished, namely HDA and VHDA. Also at 1 bar two amorphous states of ice need to be distinguished, namely LDA and HDA.

At intermediate pressure, *e.g.*, 0.5 GPa (middle panel of Fig. 8), the experimental evidence supports the existence of three amorphous "phases". Both LDA and VHDA seem to be metastable with respect to HDA, and both of them might transform to HDA. In compression experiments LDA transforms at ~120 K to HDA at 0.5 GPa.[53] VHDA transforms back to HDA-like states in isochoric experiments at intermediate pressure.[48] It is unclear whether isothermal experiments involving decompression of VHDA to 0.5 GPa result in full conversion to HDA. Decompression at 140 K does not show back-transformation to HDA at 0.5 GPa.[45] Instead the VHDA state remains after this procedure, which indicates that there is a significant barrier for the VHDA → HDA transformation at 0.5 GPa. However, we assume that the back-transformation might take place at 150 K and 0.5 GPa. Of course, more *in situ* studies are required for further addressing and refining the question relating to the transformation temperature of amorphous ices at intermediate pressure. For example *in situ* calorimetry, diffraction or dilatometry studies are suitable tools for this purpose.

For the time being, the data currently available suggest the existence of three amorphous ice "phases". This conclusion is based essentially on the data shown in Fig. 5–7. Please note that one does not require the observation of a first-order transition for distinguishing between two different amorphous ices. We do require, however, a transition, which is complete in a finite and rather sharp interval of pressure and/or temperature. Currently, we do not see any hint in the literature relating to the discovery of a fourth form of amorphous ice. On the high-pressure end VHDA was shown to transform to ice VII and ice VIII at *ca.* 3–4 GPa,[112] and on the low-pressure end LDA crystallizes to ice I. Whether or not LDA may transform to "very low density amorphous ice" (VLDA) when stretched to considerable negative pressure at 140–150 K is a proposition that remains to be explored.

## Summary

Enumerating the number of clearly distinguishable amorphous ices is a challenging issue: they lack long-range order by definition and typically relax slowly, even at 100 K. Their non-equilibrium nature prevents strict application of either the term phase or the application of the concept of a first-order transition. However, because of the metastable character and the possibility to move back and forth between amorphous ices in compression–decompression cycles, both of the above terms have been used in the literature. The plot of density *versus* pressure (Fig. 5) for well relaxed amorphous ices suggests the existence of three amorphous ices, namely LDA, HDA and VHDA. Moreover, the occurrence of (reversible) transitions in a rather narrow temperature or pressure interval between these forms suggests that a distinction between three amorphous ice "phases" should be made. Nevertheless, probably an endless number of differently relaxed states, differing, *e.g.*, in terms of density or radial distribution functions, may be obtained experimentally. On present evidence, however, these appear to be referable to as "substates" of one of the three forms: LDA, HDA or VHDA. Care needs to be taken when trying to answer the title question on the sole basis of experiments conducted at ambient pressure (Fig. 8).

 

## Acknowledgements

We are grateful to the European Research Council (ERC Starting Grant SULIWA to T.L.), the Austrian Science Fund (FWF START award Y391 to T.L. and Hertha-Firnberg fellowship to K.W.) and the Austrian Academy of Sciences (ÖAW DOC-fellowship to M.S.) for financial support.

## References

1 J. Bernstein, *Polymorphism in Molecular Crystals*, Oxford University Press, Oxford, UK, 2002.
2 M. H. Klaproth, *Bergmannische J.*, 1798, **I**, 294.
3 E. Mitscherlich, *Abh. Akad. Berlin*, 1822–1823, 43.
4 O. Mishima, L. D. Calvert and E. Whalley, *Nature*, 1985, **314**, 76.
5 M. C. Bellissent-Funel, *Europhys. Lett.*, 1998, **42**, 161.
6 E. G. Ponyatovsky and V. V. Sinitsyn, *Phys. B*, 1999, **265**, 121.
7 I. Brovchenko, A. Geiger and A. Oleinikova, *J. Chem. Phys.*, 2003, **118**, 9473.
8 P. H. Poole, F. Sciortino, U. Essmann and H. E. Stanley, *Nature*, 1992, **360**, 324.
9 H. E. Stanley, C. A. Angell, U. Essmann, M. Hemmati, P. H. Poole and F. Sciortino, *Phys. A*, 1994, **206**, 1.
10 O. Mishima and H. E. Stanley, *Nature*, 1998, **392**, 164.
11 O. Mishima, *Phys. Rev. Lett.*, 2000, **85**, 334.
12 P. G. Debenedetti, *J. Phys.: Condens. Matter*, 2003, **15**, R1669.
13 C. A. Angell, *Annu. Rev. Phys. Chem.*, 2004, **55**, 559.
14 E. A. Zheligovskaya and G. G. Malenkov, *Russ. Chem. Rev.*, 2006, **75**, 57.
15 T. Loerting, V. V. Brazhkin and T. Morishita, *Adv. Chem. Phys.*, 2009, **143**, 29.
16 T. Loerting and N. Giovambattista, *J. Phys.: Condens. Matter*, 2006, **18**, R919.
17 G. Malenkov, *J. Phys.: Condens. Matter*, 2009, **21**, 283101.
18 A. D. Fortes, I. G. Wood, L. Vocadlo, K. S. Knight, W. G. Marshall, M. G. Tucker and F. Fernandez-Alonso, *J. Appl. Crystallogr.*, 2009, **42**, 846.
19 A. D. Fortes and M. Choukroun, *Space Sci. Rev.*, 2010, **153**, 185.
20 H. E. Stanley, S. V. Buldyrev, M. Canpolat, O. Mishima, M. R. Sadr-Lahijany, A. Scala and F. W. Starr, *Phys. Chem. Chem. Phys.*, 2000, **2**, 1551.
21 S. C. Mossop, *Proc. Phys. Soc., London, Sect. B*, 1955, **68**, 193.
22 C. A. Angell, J. Shuppert and J. C. Tucker, *J. Phys. Chem.*, 1973, **77**, 3092.
23 H. Kanno, R. J. Speedy and C. A. Angell, *Science*, 1975, **189**, 880.
24 J. Swenson, R. Bergman and S. Longeville, *J. Non-Cryst. Solids*, 2002, **307–310**, 573.
25 F. Mallamace, M. Broccio, C. Corsaro, A. Faraone, U. Wanderlingh, L. Liu, C. Y. Mou and S. H. Chen, *J. Chem. Phys.*, 2006, **124**, 161102.
26 J. M. Zanotti, M. C. Bellissent-Funel and S. H. Chen, *Europhys. Lett.*, 2005, **71**, 91.
27 S. H. Chen, L. Liu, X. Chu, Y. Zhang, E. Fratini, P. Baglioni, A. Faraone and E. Mamontov, *J. Chem. Phys.*, 2006, **125**, 171103.
28 J. Swenson, H. Jansson and R. Bergman, *Phys. Rev. Lett.*, 2006, **96**, 247802.
29 K. Morishige and K. Nobuoka, *J. Chem. Phys.*, 1997, **107**, 6965.
30 S. Maruyama, K. Wakabayashi and M. Oguni, *AIP Conf. Proc.*, 2004, **708**, 675.
31 W. Kauzmann, *Chem. Rev.*, 1948, **43**, 219.
32 G. P. Johari, A. Hallbrucker and E. Mayer, *Nature*, 1987, **330**, 552.
33 M. S. Elsaesser, K. Winkel, E. Mayer and T. Loerting, *Phys. Chem. Chem. Phys.*, 2010, **12**, 708.
34 M. Seidl, M. S. Elsaesser, K. Winkel, G. Zifferer, E. Mayer and T. Loerting, *Phys. Rev. B: Condens. Matter Mater. Phys.*, 2011, in press.
35 J. S. Tse, *J. Chem. Phys.*, 1992, **96**, 5482.
36 J. S. Tse, D. D. Klug, C. A. Tulk, I. Swainson, E. C. Svensson, C. K. Loong, V. Shpakov, V. R. Belosludov, R. V. Belosludov and Y. Kawazoe, *Nature*, 1999, **400**, 647.
37 H. Schober, M. M. Koza, A. Tolle, C. Masciovecchio, F. Sette and F. Fujara, *Phys. Rev. Lett.*, 2000, **85**, 4100.
38 M. M. Koza, H. Schober, B. Geil, M. Lorenzen and H. Requardt, *Phys. Rev. B: Condens. Matter Mater. Phys.*, 2004, **69**, 024204.
39 J. L. Finney, A. Hallbrucker, I. Kohl, A. K. Soper and D. T. Bowron, *Phys. Rev. Lett.*, 2002, **88**, 225503.
40 E. F. Burton and W. F. Oliver, *Proc. R. Soc. London, Ser. A*, 1935, **153**, 166.
41 E. F. Burton and W. F. Oliver, *Nature*, 1935, **135**, 505.
42 D. T. Bowron, J. L. Finney, A. Hallbrucker, I. Kohl, T. Loerting, E. Mayer and A. K. Soper, *J. Chem. Phys.*, 2006, **125**, 194502.
43 E. Mayer, *J. Appl. Phys.*, 1985, **58**, 663.
44 K. Winkel, D. T. Bowron, T. Loerting, E. Mayer and J. L. Finney, *J. Chem. Phys.*, 2009, **130**, 204502.
45 K. Winkel, M. S. Elsaesser, E. Mayer and T. Loerting, *J. Chem. Phys.*, 2008, **128**, 044510.
46 K. Winkel, M. S. Elsaesser, M. Seidl, M. Bauer, E. Mayer and T. Loerting, *J. Phys.: Condens. Matter*, 2008, **20**, 494212.
47 O. Mishima, L. D. Calvert and E. Whalley, *J. Phys. Colloq.*, 1984, **C8**, 239.
48 T. Loerting, C. Salzmann, I. Kohl, E. Mayer and A. Hallbrucker, *Phys. Chem. Chem. Phys.*, 2001, **3**, 5355.
49 R. J. Nelmes, J. S. Loveday, T. Straessle, C. L. Bull, M. Guthrie, G. Hamel and S. Klotz, *Nat. Phys.*, 2006, **2**, 414.
50 O. Mishima, *J. Chem. Phys.*, 1994, **100**, 5910.
51 C. G. Salzmann, T. Loerting, S. Klotz, P. W. Mirwald, A. Hallbrucker and E. Mayer, *Phys. Chem. Chem. Phys.*, 2006, **8**, 386.
52 T. Loerting, W. Schustereder, K. Winkel, C. G. Salzmann, I. Kohl and E. Mayer, *Phys.Rev. Lett.*, 2006, **96**, 025702.
53 K. Winkel, W. Schustereder, I. Kohl, C. G. Salzmann, E. Mayer and T. Loerting, in *Proc. 11th Intl. Conf. on the Physics and Chemistry of Ice*, ed. W. F. Kuhs, RSC, Dorchester, UK, 2007, p. 641.
54 O. Mishima, *Nature*, 1996, **384**, 546.
55 C. G. Venkatesh, S. A. Rice and A. H. Narten, *Science*, 1974, **186**, 927.
56 E. Mayer and R. Pletzer, *Nature*, 1986, **319**, 298.
57 R. Pletzer and E. Mayer, *J. Chem. Phys.*, 1989, **90**, 5207.
58 P. Ayotte, R. S. Smith, K. P. Stevenson, Z. Dohnalek, G. A. Kimmel and B. D. Kay, *J. Geophys. Res.*, 2001, **106**, 33387.
59 E. Mayer and R. Pletzer, *J. Phys. Colloq.*, 1987, **48**, 581.
60 J. Klinger, *J. Phys. Colloq.*, 1985, **C8**, 657.
61 P. Jenniskens and D. F. Blake, *Science*, 1994, **265**, 753.
62 P. Jenniskens and D. F. Blake, *Astrophys. J.*, 1996, **473**, 1104.
63 P. Jenniskens and D. F. Blake, *Planet. Space Sci.*, 1996, **44**, 711.
64 M. E. Palumbo, G. A. Baratta, G. Leto and G. Strazzulla, *J. Mol. Struct.*, 2010, **972**, 64.
65 D. S. Olander and S. A. Rice, *Proc. Natl. Acad. Sci. U. S. A.*, 1972, **69**, 98.
66 E. Mayer and R. Pletzer, *J. Chem. Phys.*, 1984, **80**, 2939.
67 G. A. Kimmel, Z. Dohnalek, K. P. Stevenson, R. S. Smith and B. D. Kay, *J. Chem. Phys.*, 2001, **114**, 5295.
68 G. A. Kimmel, K. P. Stevenson, Z. Dohnalek, R. S. Smith and B. D. Kay, *J. Chem. Phys.*, 2001, **114**, 5284.
69 Z. Dohnalek, G. A. Kimmel, P. Ayotte, R. S. Smith and B. D. Kay, *J. Chem. Phys.*, 2003, **118**, 364.
70 E. Mayer, *J. Phys. Chem.*, 1985, **89**, 3474.
71 M. G. Sceats and S. A. Rice, in *Water, a Comprehensive Treatise*, ed. F. Franks, Plenum Press, New York, 1982, vol. 7, p. 83.
72 A. Hallbrucker, E. Mayer and G. P. Johari, *J. Phys. Chem.*, 1989, **93**, 4986.
73 M. Fisher and J. P. Devlin, *J. Phys. Chem.*, 1995, **99**, 11584.
74 M. Chonde, M. Brindza and V. Sadtchenko, *J. Chem. Phys.*, 2006, **125**, 094501.
75 S. M. McClure, E. T. Barlow, M. C. Akin, D. J. Safarik, T. M. Truskett and C. B. Mullins, *J. Phys. Chem. B*, 2006, **110**, 17987.
76 S. M. McClure, D. J. Safarik, T. M. Truskett and C. B. Mullins, *J. Phys. Chem. B*, 2006, **110**, 11033.
77 J. Zarzycki, *Glasses and the vitreous state*, Cambridge University Press, Cambridge, UK, 1991.
78 A. Eisenberg, in *Physical Properties of Polymers*, ed. A. E. James, E. Mark, W. W. Graessley, L. Mandelkern, E. T. Samulski, J. L. Koenig and G. D. Wignall, American Chemical Society, Washington, DC, 1993.
79 P. Brüggeller and E. Mayer, *Nature*, 1980, **288**, 569.
80 E. Mayer and P. Brüggeller, *Nature*, 1982, **298**, 715.
81 O. Mishima, L. D. Calvert and E. Whalley, *Nature*, 1984, **310**, 393.

82 T. Loerting, I. Kohl, W. Schustereder, A. Hallbrucker and E. Mayer, *ChemPhysChem*, 2006, **7**, 1203.
83 Y. P. Handa, O. Mishima and E. Whalley, *J. Chem. Phys.*, 1986, **84**, 2766.
84 D. D. Klug, Y. P. Handa, J. S. Tse and E. Whalley, *J. Chem. Phys.*, 1989, **90**, 2390.
85 A. I. Kolesnikov, V. V. Sinitsyn, E. G. Ponyatovsky, I. Natkaniec, L. S. Smirnov and J. C. Li, *J. Phys. Chem. B*, 1997, **101**, 6082.
86 Y. Yoshimura, S. T. Stewart, M. Somayazulu, H.-k. Mao and R. J. Hemley, *J. Chem. Phys.*, 2006, **124**, 024502.
87 C. McBride, C. Vega, E. Sanz and J. L. F. Abascal, *J. Chem. Phys.*, 2004, **121**, 11907.
88 Y. Yoshimura, H.-k. Mao and R. J. Hemley, *Chem. Phys. Lett.*, 2006, **420**, 503.
89 N. Sartori, J. Bednar and J. Dubochet, *J. Microsc.*, 1996, **182**, 163.
90 G. A. Baratta, G. Leto, F. Spinella, G. Strazzulla and G. Foti, *Astron. Astrophys.*, 1991, **252**, 421.
91 A. Kouchi and T. Kuroda, *Nature*, 1990, **344**, 134.
92 G. Leto and G. A. Baratta, *Astron. Astrophys.*, 2003, **397**, 7.
93 J. L. Finney, D. T. Bowron, A. K. Soper, T. Loerting, E. Mayer and A. Hallbrucker, *Phys. Rev. Lett.*, 2002, **89**, 205503.
94 A. K. Soper, *Chem. Phys.*, 1996, **202**, 295.
95 A. K. Soper, *Phys. Rev. B: Condens. Matter Mater. Phys.*, 2005, **72**, 104204.
96 S. Klotz, T. Straessle, A. M. Saitta, G. Rousse, G. Hamel, R. J. Nelmes, J. S. Loveday and M. Guthrie, *J. Phys.: Condens. Matter*, 2005, **17**, S967.
97 G. P. Johari, *J. Chem. Educ.*, 1974, **51**, 23.
98 S. F. Swallen, K. L. Kearns, M. K. Mapes, Y. S. Kim, R. J. McMahon, M. D. Ediger, T. Wu, L. Yu and S. Satija, *Science*, 2007, **315**, 353.
99 K. L. Kearns, S. F. Swallen, M. D. Ediger, T. Wu and L. Yu, *J. Chem. Phys.*, 2007, **127**, 154702.
100 C. A. Angell, *Phys. D*, 1997, **107**, 122.
101 C. A. Tulk, C. J. Benmore, J. Urquidi, D. D. Klug, J. Neuefeind, B. Tomberli and P. A. Egelstaff, *Science*, 2002, **297**, 1320.
102 M. Guthrie, J. Urquidi, C. A. Tulk, C. J. Benmore, D. D. Klug and J. Neuefeind, *Phys. Rev. B: Condens. Matter Mater. Phys.*, 2003, **68**, 184110.
103 M. M. Koza, H. Schober, H. E. Fischer, T. Hansen and F. Fujara, *J. Phys.: Condens. Matter*, 2003, **15**, 321.
104 Y. Suzuki and Y. Tominaga, *J. Chem. Phys.*, 2010, **133**, 164508.
105 T. Loerting, C. G. Salzmann, K. Winkel and E. Mayer, *Phys. Chem. Chem. Phys.*, 2006, **8**, 2810.
106 H. Schober, M. Koza, A. Tölle, F. Fujara, C. A. Angell and R. Böhmer, *Phys. B*, 1998, **241–243**, 897.
107 O. Mishima and Y. Suzuki, *Nature*, 2002, **419**, 599.
108 E. L. Gromnitskaya, O. V. Stal'gorova, A. G. Lyapin, V. V. Brazhkin and O. B. Tarutin, *JETP Lett.*, 2003, **78**, 488.
109 M. M. Koza, T. Hansen, R. P. May and H. Schober, *J. Non-Cryst. Solids*, 2006, **352**, 4988.
110 M. Scheuermann, B. Geil, K. Winkel and F. Fujara, *J. Chem. Phys.*, 2006, **124**, 224503.
111 M. M. Koza, B. Geil, K. Winkel, C. Koehler, F. Czeschka, M. Scheuermann, H. Schober and T. Hansen, *Phys. Rev. Lett.*, 2005, **94**, 125506.
112 S. Klotz, G. Hamel, J. S. Loveday, R. J. Nelmes and M. Guthrie, *Z. Kristallogr.*, 2003, **218**, 117.




 